

Schur Decomposition for Stiff Differential Equations

Thoma Zoto · John C. Bowman

Submitted: May 13, 2023

Abstract A quantitative definition of numerical stiffness for initial value problems is proposed. Exponential integrators can effectively integrate linearly stiff systems, but they become expensive when the linear coefficient is a matrix, especially when the time step is adapted to maintain a prescribed local error. Schur decomposition is shown to avoid the need for computing matrix exponentials in such simulations, while still circumventing linear stiffness.

Keywords exponential integrators · stiff differential equations · numerical stiffness · Schur decomposition · Runge–Kutta methods

Mathematics Subject Classification (2020) 65L04 · 65L06 · 65M22

1 Introduction

The time integration of initial value problems is ubiquitous in simulations of physical phenomena. Consider a first-order initial value problem of the form

$$\frac{dy}{dt} = f(t, y(t)) = F(t, y(t)) - Ly, \quad y(0) = y_0, \quad (1)$$

where y is a vector, F is an analytic function, and L is a constant matrix. Numerical approximations of a future estimate y_{n+1} can be obtained using an

Financial support for this work was provided by grants RES0043585 and RES0046040 from the Natural Sciences and Engineering Research Council of Canada.

T. Zoto
RAPSODI, Inria Lille–Nord Europe, Villeneuve d’Ascq 59650, France
E-mail: thomazoto1@gmail.com

J.C. Bowman
Department of Mathematical and Statistical Sciences, University of Alberta, Edmonton,
Alberta T6G 2G1, Canada
E-mail: bowman@ualberta.ca

explicit Runge–Kutta (RK) method:

$$y_n^{i+1} = y_n^0 + h \sum_{j=0}^i a_{ij} f(t_n + c_j h, y_n^j) \quad i = 0, \dots, s-1, \quad (2)$$

where $n = 0, 1, \dots$, $y_0^0 = y_0$, $y_n^s = y_{n+1}$, h is the *time step*, $t_n = nh$, a_{ij} are the Runge–Kutta *weights*, and c_j are the *step fractions* for stage j . For $n \geq 1$, $y_n^0 = y_{n-1}^s$ is the approximation of the solution at time nh , also denoted by y_n . It is customary to organize the weights in a *Butcher tableau* (Table 1). For some

0				
c_1	a_{00}			
c_2	a_{10}	a_{11}		
\vdots	\vdots	\vdots	\ddots	
c_{s-1}	$a_{(s-2)0}$	\cdots	\cdots	$a_{(s-2)(s-2)}$
1	$a_{(s-1)0}$	\cdots	\cdots	$a_{(s-1)(s-1)}$

Table 1: General Runge–Kutta tableau

problems, explicit Runge–Kutta methods may require a very small time step. This failure is often called numerical stiffness, and is described and defined in Section 2. While one might consider implicit methods, they require iteration within a time step. Exponential Runge–Kutta (ERK) integrators provide an alternative to implicit methods for solving stiff problems. These are explicit methods that alleviate the burden of stiffness and have similar structure to explicit Runge–Kutta methods (a notable difference being that the weights are not constants, but depend on the matrix L):

$$y_n^{i+1} = e^{-hL} y_n^0 + h \sum_{j=0}^i a_{ij} (-hL) F(t_n + c_j h, y_n^j) \quad i = 0, \dots, s-1. \quad (3)$$

We briefly describe these methods in Section 3. In Section 4, we show how Schur decomposition can be used to improve the efficiency of exponential integrators when L is a nondiagonal matrix. We conclude the paper with some numerical examples and applications in Section 5.

2 Stiffness of Explicit Methods

We focus on solving ordinary differential equations (ODEs) or systems of ODEs of the form (1). In practical applications, such systems of ODEs arise upon spatial discretization of a PDE via finite differences, finite elements, or spectral transforms.

One of the most common ways of quantifying stiffness in the literature is the concept of the *stiffness ratio*. If we denote λ_{\min} and λ_{\max} to be the smallest and the largest eigenvalues of L (in modulus), then the stiffness ratio is

$$\frac{|\operatorname{Re} \lambda_{\max}|}{|\operatorname{Re} \lambda_{\min}|}. \quad (4)$$

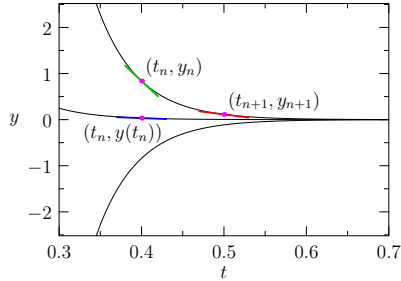
The larger this ratio is, the more stiff the system is considered to be. However, many authors have realized that this is not the best definition for the phenomena because, if λ_{\min} is zero, then the stiffness ratio is infinite, but the problem may not be stiff at all. Lambert describes a few other attempts to define stiffness based on stability, accuracy, or decay rates, although none of them are satisfactory, either due to the existence of a counterexample or due to their qualitative rather than quantitative nature [10]. One statement that Lambert seems to accept (and one that has also been used consistently in the literature alongside the stiffness ratio) is:

Statement 1 *If a numerical method with a finite region of absolute stability, applied to a system with any initial conditions, is forced to use in a certain interval of integration a step-length which is excessively small in relation to the smoothness of the exact solution in that interval, then the system is said to be stiff in that interval.*

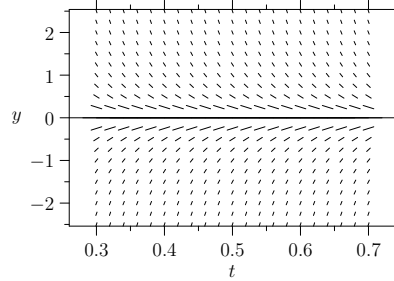
This is a helpful definition if we want to just know by testing whether a system is stiff or not, but it requires actually applying a method and observing whether it fails. Typically, stiff systems are solved numerically by first trying an explicit method and, if that fails for reasonable step sizes, switching to an implicit method. Understood in this way, Statement 1 portrays stiffness as a property that depends on the chosen numerical method and not as an intrinsic phenomenon of the ODE system itself. We want to define stiffness so that it depends only on the ODE system and is helpful for applying exponential integrators, distinguishing between stiffness coming from a linear term and stiffness coming from a nonlinear term.

In order to gain some insights about stiffness, let us first explore how explicit and implicit methods solve ODEs. We recall the two simplest time integrating schemes: the explicit Euler method $y_{n+1} = y_n + hf(y_n)$ and implicit Euler method $y_{n+1} = y_n + hf(y_{n+1})$. In Figure 1a, we present a graphical description of why the explicit Euler method performs poorly when $F(t, y(t)) = 0$, $L = 20$ and $y_0 = 1$ in (1). At each time t_n , these methods compute an approximation to the exact solution that lies on a nearby solution curve. The implicit Euler method evolves the solution in the direction of the tangent line to the nearby solution curve at the point (t_{n+1}, y_{n+1}) (red segment), while the explicit Euler method evolves in the direction of the tangent line to the nearby solution curve at the point (t_n, y_n) (green segment). The tangent line at (t_{n+1}, y_{n+1}) is much closer to the direction of the exact solution at the point $(t_n, y(t_n))$, unlike the tangent line at (t_n, y_n) . The bigger the step size, the more aligned the tangent line at (t_{n+1}, y_{n+1}) will be with the direction of the exact solution at the point $(t_n, y(t_n))$, in contrast to the tangent line

at (t_n, y_n) . This phenomenon causes the explicit Euler method to work only for sufficiently small step sizes. The corresponding slope field is shown in Figure 1b.



(a) Graphical interpretation of explicit and implicit Euler methods.



(b) Slope field of $\frac{dy}{dt} = -20y$.

This point of view on stiffness can also be extended to general systems of ODEs. It was first introduced by [5] and described by [10]. We will expand on these ideas to make them applicable to the stiff differential equations that we aim to solve with exponential integrators. We borrow the following two systems from [10]:

System 1:

$$\begin{bmatrix} y_1' \\ y_2' \end{bmatrix} = \begin{bmatrix} -2 & 1 \\ 1 & -2 \end{bmatrix} \begin{bmatrix} y_1 \\ y_2 \end{bmatrix} + \begin{bmatrix} 2 \sin(t) \\ 2(\cos(t) - \sin(t)) \end{bmatrix}, \quad \begin{bmatrix} y_1(0) \\ y_2(0) \end{bmatrix} = \begin{bmatrix} 2 \\ 3 \end{bmatrix}, \quad (5)$$

System 2:

$$\begin{bmatrix} y_1' \\ y_2' \end{bmatrix} = \begin{bmatrix} -2 & 1 \\ 998 & -999 \end{bmatrix} \begin{bmatrix} y_1 \\ y_2 \end{bmatrix} + \begin{bmatrix} 2 \sin(t) \\ 999(\cos(t) - \sin(t)) \end{bmatrix}, \quad \begin{bmatrix} y_1(0) \\ y_2(0) \end{bmatrix} = \begin{bmatrix} 2 \\ 3 \end{bmatrix}. \quad (6)$$

The particular solution for the given initial conditions is the same for **System 1** and **System 2**:

$$\begin{bmatrix} y_1(t) \\ y_2(t) \end{bmatrix} = 2 \exp(-t) \begin{bmatrix} 1 \\ 1 \end{bmatrix} + \begin{bmatrix} \sin(t) \\ \cos(t) \end{bmatrix}. \quad (7)$$

Lambert selected the initial condition $y(0) = [2, 3]^\top$, so that **System 1** and **System 2** have the same exact solution, to emphasize that the concept of stiffness does not depend on the particular solution. In Figure 2 we plot the components as well as the phase curves corresponding to various initial conditions for both systems, allowing one to examine nearby solutions.

As suggested by Lambert, to help us generalize the discussion of stiffness from the case of a single ODE, we zoom in on the initial evolution in Figure 3. While the nearby solutions for y_2 are seen in Figure 3c to be nearly parallel to each other for (nonstiff) **System 1**, they are seen in Figure 3d to approach each

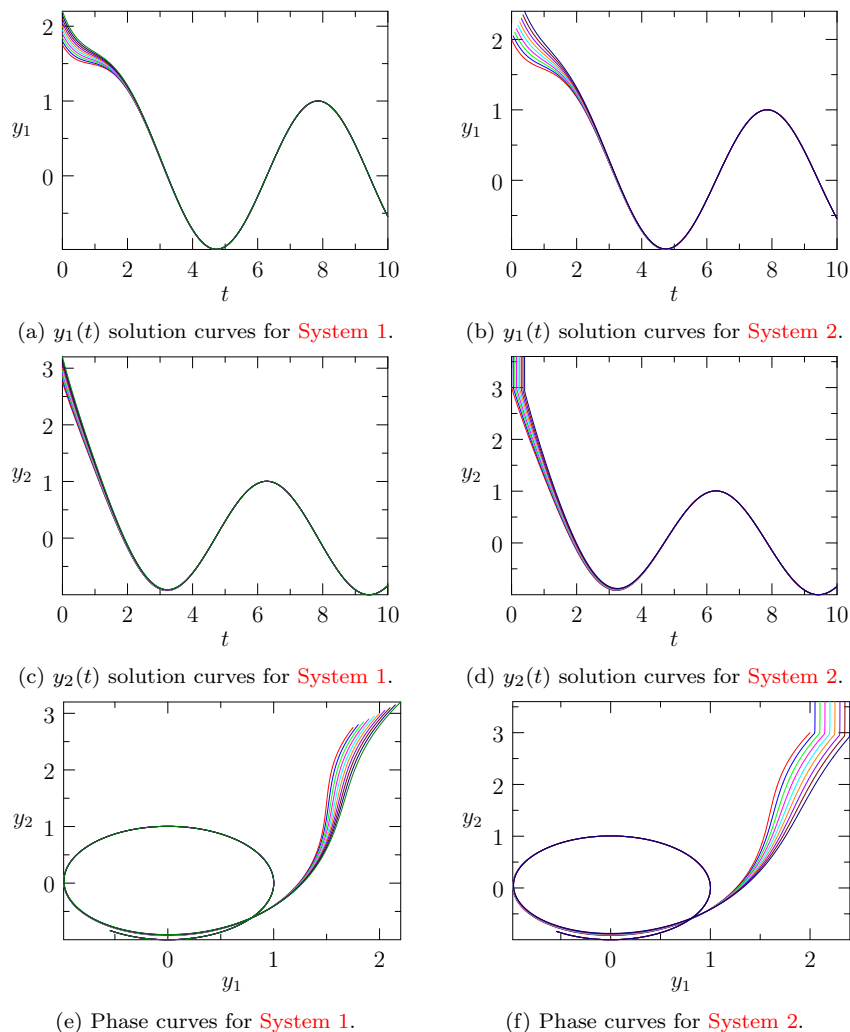


Fig. 2: Plots of nearby solution curves for **System 1** and **System 2**.

other at a steep angle for (stiff) **System 2**. This anomaly can also be observed in the phase curves of **System 2** in 3f.

For example, for some t_n , the exact value of the solution for **System 2** is $y(t_n) = [1.998, 2.99]$, while the numerical algorithm estimates it with some error as $y_n = [1.998, 3.01]$. The difference between $y(t_n)$ and y_n is negligible, but the difference between the slope field vector at $y(t_n)$ and the slope field vector at y_n is large (see Figure 4d). In contrast, the corresponding vectors in Figure 4c are closely aligned. Since these vectors form the right-hand side of the ODE at $y(t_n)$ and y_n , we see that **System 2** can pose problems for explicit

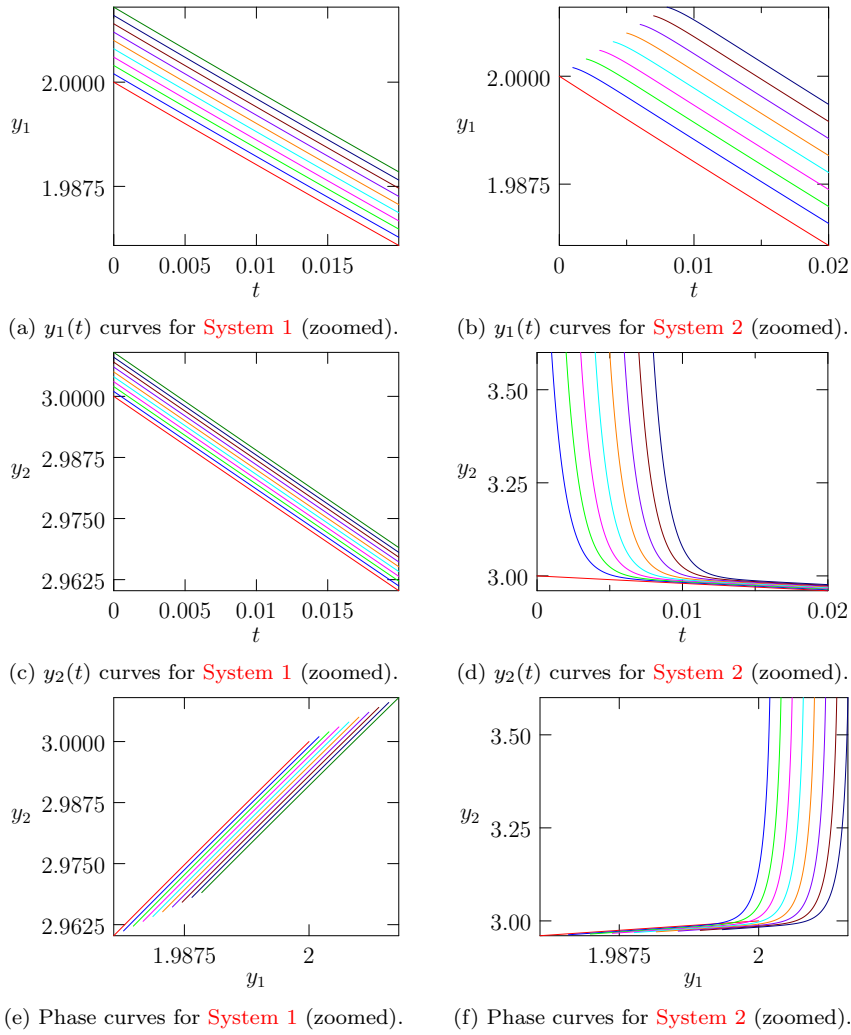


Fig. 3: Plots of nearby solution curves for **System 1** and **System 2** zoomed in.

Runge–Kutta methods. A common but inefficient remedy is to reduce the time step so that the vectors $f(t_n, y_n)$ and $f(t_n, y(t_n))$ become more aligned.

We can now investigate the last statement considered by Lambert [10] and attributed to Curtiss and Hirschfelder [5], which will eventually lead us to our ultimate definition of stiffness.

Statement 2 *A system is said to be stiff in a given interval of time if, in that interval, the neighbouring solution curves approach the solution curve at a rate which is very large in comparison with the rate at which the solution varies.*

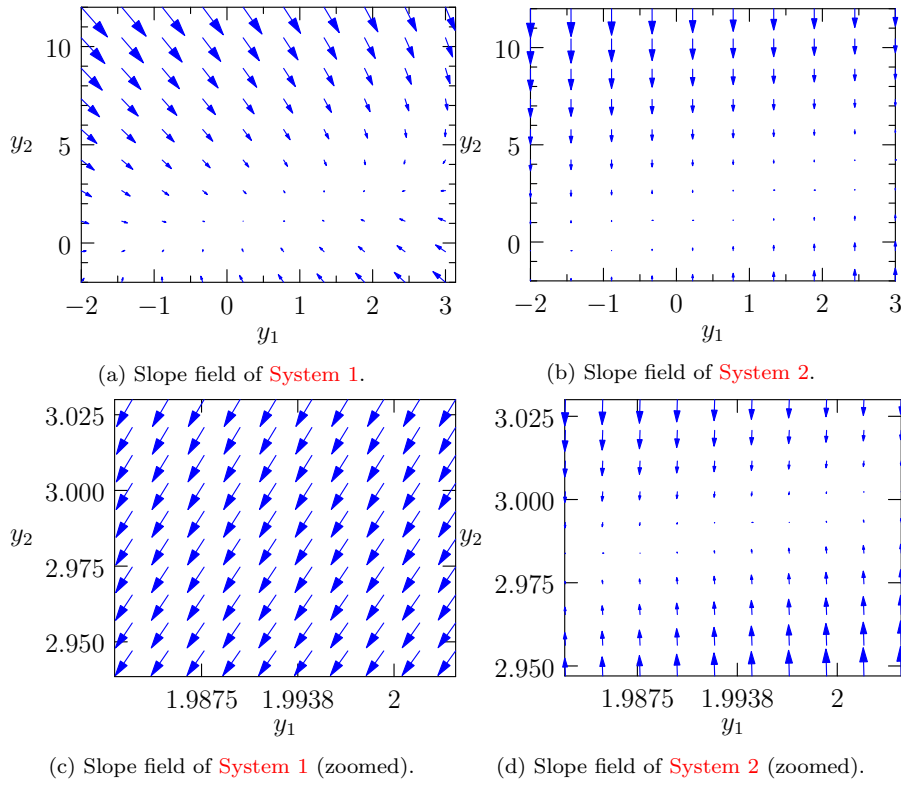


Fig. 4: Slope field plots for **System 1** and **System 2**.

As Lambert points out for Statement 1, Statement 2 also includes the idea that the stiffness of a system will depend on where in the phase space the numerical integration takes place. The reason why Lambert does not adopt Statement 2 is that it requires knowledge of at least two solutions of the system in order to decide whether nearby curves approach the desired solution curve at a fast or slow rate. Based on the connection we made to the slope field, however, we can translate the geometric phenomenon of nearby curves approaching at a fast rate to the more analytic interpretation that the function $f(t, y)$ has a large Lipschitz constant [5]:

$$\sup_{\substack{t_1 \neq t_2 \\ y_1 \neq y_2}} \frac{|f(t_1, y_1) - f(t_2, y_2)|}{|(t_1, y_1) - (t_2, y_2)|}.$$

Essentially, stiff systems are those for which “a small change in y leads to a large change in $f(t, y)$ ” [10]. Lambert argues against this statement as well since it is not apparent what critical value the Lipschitz constant should be compared to. The original interest in defining stiffness was solely to avoid wasting limited resources in solving stiff systems with explicit methods. However, we

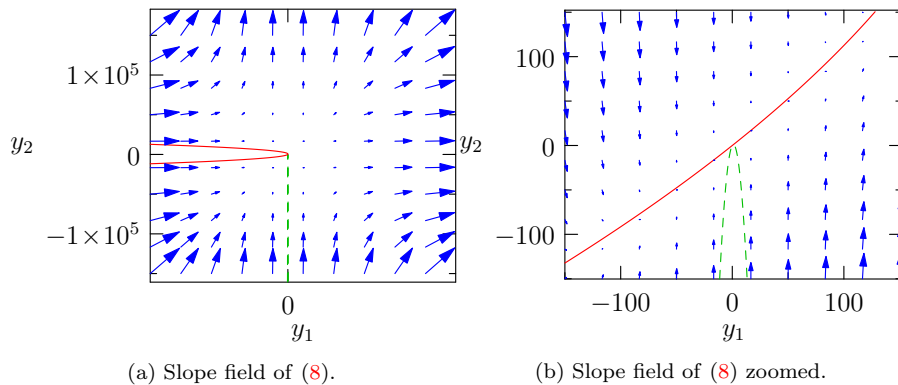


Fig. 5: Slope field plots of (8) showing the fixed curves C_1 (dashed green) and C_2 (solid red).

are interested in refining the definition of stiffness further to allow us to specifically detect linear stiffness (numerical stiffness coming from the linear source term of the ODE system), so that we can apply exponential integrators as needed.

Curtiss and Hirschfelder [5] attribute stiffness in a one-dimensional system to a drastic change in the slope field across a particular solution curve. Generalizing this idea to two dimensions, we consider the equation

$$\begin{bmatrix} y_1' \\ y_2' \end{bmatrix} = \begin{bmatrix} -2 & 1 \\ 998 & -999 \end{bmatrix} \begin{bmatrix} y_1 \\ y_2 \end{bmatrix} + \begin{bmatrix} y_1^2 \\ y_2^2 \end{bmatrix}. \quad (8)$$

The solution lives in a three-dimensional space, with the axes being t , y_1 , and y_2 . We first identify the *fixed curves* of the components of the system of ODEs (8): denote by C_1 the curve corresponding to $dy_1/dt = 0$ and by C_2 the curve corresponding to $dy_2/dt = 0$. Pick one of them, say C_2 . Fix y_1 and calculate the corresponding y_2 from the equation for C_2 . Consider some test values $\tilde{y}_{2a} \in (y_2 - \varepsilon, y_2)$ and $\tilde{y}_{2b} \in (y_2, y_2 + \varepsilon)$ for some sufficiently small ε . The system is stiff if the slope field vector at (y_1, \tilde{y}_{2a}) or (y_1, \tilde{y}_{2b}) is not aligned with the slope field vector at (y_1, y_2) . We repeat the process for C_1 . The equations for C_1 and C_2 are

$$C_1 : \quad 0 = -2y_1 + y_2 + y_1^2, \quad (9)$$

$$C_2 : \quad 0 = 998y_1 - 999y_2 + y_2^2. \quad (10)$$

We plot these curves and the slope field in Figure 5. We note in this case that stiffness manifests itself only in some parts of the phase space: *stiffness can be a local phenomenon*.

In contrast, the system obtained by removing the nonlinear terms from (8),

$$\begin{bmatrix} y_1' \\ y_2' \end{bmatrix} = \begin{bmatrix} -2 & 1 \\ 998 & -999 \end{bmatrix} \begin{bmatrix} y_1 \\ y_2 \end{bmatrix}, \quad (11)$$

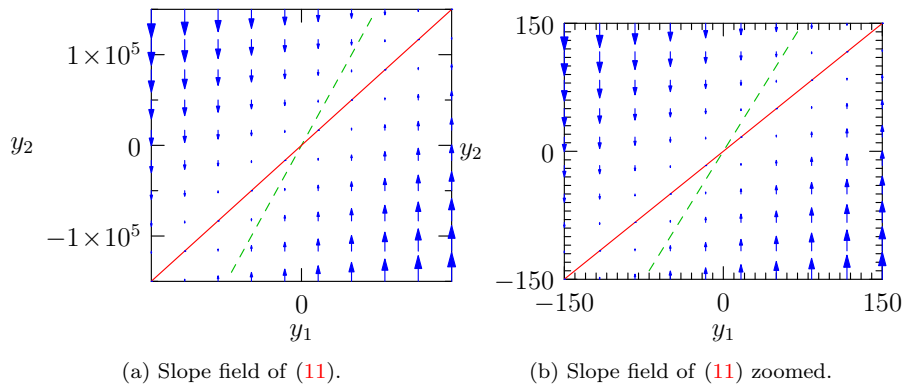


Fig. 6: Slope field plots of (11) showing the fixed curves C_1 (dashed green) and C_2 (solid red).

becomes stiff for every initial condition. Here, the equations for the curves C_1 and C_2 are

$$C_1 : \quad 0 = -2y_1 + y_2, \quad (12)$$

$$C_2 : \quad 0 = 998y_1 - 999y_2; \quad (13)$$

these are plotted together with the corresponding slope field in Figure 6. This is another confirmation that stiffness cannot be measured by properties of the linear operator only and makes it crucial to have a definition that can recognize if the equation is stiff or not in the phase space region of interest.

The idea of testing the behaviour of the source function near fixed curves provides a fast but heuristic way of determining if an equation is stiff in a particular region. However, Cartwright has proposed an alternative, more theoretical, definition of stiffness based on local Lyapunov exponents and curvature [2]. Although he is mostly concerned with defining stiffness in chaotic systems, part of his work aligns well with the discussion here. In fact, we consider Cartwright's definition to be the preferred definition of stiffness as it is local and provides a way of quantifying the rate at which nearby solution curves approach the exact solution.

Stiff systems can be recognized by how fast nearby solutions approach a fixed curve and, as mentioned above, what characterizes the rate of separation or contraction of solution curves of a system of ODEs are the Lyapunov exponents. Since Lyapunov exponents give a global picture of the phase space, to investigate what happens locally we will need *local Lyapunov exponents*. Let $\sigma_i(t)$ be the principal axes of an ellipsoidal ball evolving in time in phase space. The i^{th} local Lyapunov exponent is

$$\gamma_i(\tau, t) = \lim_{\sigma_i(\tau) \rightarrow 0} \frac{1}{\tau} \log \frac{\sigma_i(t + \tau)}{\sigma_i(t)}. \quad (14)$$

We hinted earlier that while nearby solutions play a major role in detecting stiffness in a system of ODEs, the wiggleness of the solution curve at the

section of interest in the phase space also plays an important role. Cartwright quantifies the latter by using the curvature $\kappa = y''(1 + y'^2)^{-3/2}$ of the solution y . Cartwright states that “a system is stiff in a given interval if in that interval the most negative local Lyapunov exponent is large, while the curvature of the solution is small” [2]. He quantifies stiffness by the ratio

$$R_{nl} = \frac{\left| \min_{1 \leq i \leq n} \gamma_i(\tau, t) \right|}{\kappa(t)}, \quad (15)$$

but he does not compare the ratio to anything and hence leaves it open to Lambert’s argument against Statement 2.

Cartwright also points out that the ratio R_{nl} could be averaged over the trajectory to yield a global measure of stiffness, but we have already seen that stiffness can be a local phenomenon. Therefore, we slightly modify Cartwright’s definition to

Definition 1 A system is *stiff* in a given interval if in that interval the most negative local Lyapunov exponent is much larger in absolute value than the curvature of the solution curve.

In the remainder of this work, we focus on systems of ODEs of the form (1), such that the stiffness in the sense of Definition 1 stems mostly from the term Ly .

3 Exponential Integrators

We now introduce a class of methods known as *exponential integrators*, first encountered in [3], that avoid linear stiffness by treating the linear term exactly.

Returning to (1), we define the function $G(t) = F(t, y(t))$, and introduce the integrating factor $t \mapsto e^{tL}$. As shown in [13], a change of both independent and dependent variables allows us to write the exact solution of (1) as

$$y(t_n + h) = e^{-hL}y(t_n) + \sum_{k=0}^{\infty} h^{k+1} \varphi_{k+1}(-hL) G^{(k)}(t_n), \quad (16)$$

where

$$\varphi_k(0) = \frac{1}{k!}, \quad (17)$$

$$\varphi_0(x) = e^x, \quad (18)$$

$$\varphi_{k+1}(x) = \frac{\varphi_k(x) - \frac{1}{k!}}{x} \text{ for } k \geq 0. \quad (19)$$

Note that (16) agrees with equation (4.6) of Ref. [7] obtained by applying the variation-of-constants method to (1) and Taylor expanding G .

Exponential Runge–Kutta methods approximate the infinite sum and derivatives of G in (16). The simplest approximation, called the exponential Euler method, truncates the sum after the first term:

$$y(t_n + h) = \varphi_0(-hL)y_n + h\varphi_1(-hL)F(t_n, y_n). \quad (20)$$

The exponential Euler method solves (1) exactly whenever $F(t, y)$ is constant but reduces to the explicit Euler method in the *classical limit* $L \rightarrow 0$.

As shown by Hochbruck and Ostermann [7], great care must be taken when deriving a higher-order exponential integrator to ensure that it retains its design order when applied to stiff problems. Hochbruck and Ostermann demonstrate that several fourth-order exponential integrators in the literature exhibit an order reduction when applied to a particular test problem. For example, the stiff order of the scheme ETD4RK of Cox and Matthews [4] can drop from four to two. For consistency of nomenclature, we refer to this method **ERK4CM** and give its Butcher tableau in Table 2.

0				
$\frac{1}{2}$	$\frac{1}{2}\varphi_1\left(-\frac{hL}{2}\right)$			
$\frac{3}{4}$	0	$\frac{1}{2}\varphi_1\left(-\frac{hL}{2}\right)$		
1	$\frac{1}{2}\varphi_1\left(-\frac{hL}{2}\right)\left(\varphi_0\left(-\frac{hL}{2}\right) - 1\right)$	0	$\varphi_1\left(-\frac{hL}{2}\right)$	
1	$\varphi_1 - 3\varphi_2 + 4\varphi_3$	$2\varphi_2 - 4\varphi_3$	$2\varphi_2 - 4\varphi_3$	$4\varphi_3 - \varphi_2$

Table 2: ERK4CM tableau, where $\varphi_i = \varphi_i(-hL)$.

Similarly, the exponential integrator of Krogstad [9] in Table 3, which we denote **ERK4K**, can suffer an order reduction from four to three.

0				
$\frac{1}{2}$	$\frac{1}{2}\varphi_1\left(-\frac{hL}{2}\right)$			
$\frac{1}{2}$	$\frac{1}{2}\varphi_1\left(-\frac{hL}{2}\right) - \varphi_2\left(-\frac{hL}{2}\right)$	$\varphi_2\left(-\frac{hL}{2}\right)$		
1	$\varphi_1 - 2\varphi_2$	0	$2\varphi_2$	
1	$\varphi_1 - 3\varphi_2 + 4\varphi_3$	$2\varphi_2 - 4\varphi_3$	$2\varphi_2 - 4\varphi_3$	$4\varphi_3 - \varphi_2$

Table 3: ERK4K tableau, where $\varphi_i = \varphi_i(-hL)$.

Hochbruck and Ostermann [7] derived a set of stiff-order conditions that are sufficient to prevent such order reductions. They propose the five-stage method shown in Table 4, which we denote **ERK4HO5**.

State-of-the-art numerical methods use adaptive time-stepping to efficiently allocate computational resources. These methods adjust the time step to keep

0					
$\frac{1}{2}$	$\frac{1}{2}\varphi_1\left(-\frac{hL}{2}\right)$				
$\frac{1}{2}$	$\frac{1}{2}\varphi_1\left(-\frac{hL}{2}\right) - \varphi_2\left(-\frac{hL}{2}\right)$	$\varphi_2\left(-\frac{hL}{2}\right)$			
1	$\varphi_1 - 2\varphi_2$	φ_2	φ_2		
$\frac{1}{2}$	$\frac{1}{2}\varphi_1\left(-\frac{hL}{2}\right) - 2a_{31} - a_{33}$	a_{31}	a_{31}	$\frac{1}{4}\varphi_2\left(-\frac{hL}{2}\right) - a_{31}$	
1	$\varphi_1 - 3\varphi_2 + 4\varphi_3$	0	0	$-\varphi_2 + 4\varphi_3$	$4\varphi_2 - 8\varphi_3$

$$\varphi_i = \varphi_i(-hL),$$

$$a_{31} = \frac{1}{2}\varphi_2\left(-\frac{hL}{2}\right) - \varphi_3 + \frac{1}{4}\varphi_2 - \frac{1}{2}\varphi_3\left(-\frac{hL}{2}\right).$$

Table 4: ERK4HO5 tableau.

the estimated local error within prescribed bounds. The error estimate is computed as the difference between high- and low-order approximations. Embedded methods, which share some of the sample function evaluations between the two approximations, can yield very efficient adaptive time stepping schemes. As pointed out in Ref. [13], it is important that embedded method be *robust*: the order of the low-order approximation should never equal the order n of the high-order approximation for any function $G(t)$ with a nonzero derivative of order less than n . A robust fourth-order embedded exponential integrator called **ERK43ZB** is presented in Table 5 [13].

4 Schur decomposition

Exponential integrators are invariant under the transformation of (1) to the autonomous form of the equation (where f does not have an explicit time dependence), by introducing a new independent variable:

$$\frac{dy}{dt} = F(y) - Ly. \quad (21)$$

Applying an exponential Runge–Kutta method to such a system requires the evaluation of $\varphi_k(c_j hL)$ for certain values of k and j . Since L is assumed to be a general matrix, these functions are related to the matrix exponential. Methods for efficiently calculating such matrix functions, and the matrix exponential in particular, are an active field of research. In our testing, we chose to implement a scaling and squaring algorithm, followed by a Padé approximant, for calculating the matrix exponential [11][6]. Although slow, this is a reliable technique for calculating the φ_k functions for a general matrix L . In particular cases, special properties of L may be used to devise more computationally efficient methods. For example, if L is a sparse matrix, it is worth implementing a Krylov subspace method. A short description of Krylov subspace methods (as well as other methods such as Chebyshev methods, Leja

$$\begin{array}{c|cccc}
0 & & & & \\
\frac{1}{6} & \frac{1}{6}\varphi_1\left(-\frac{hL}{6}\right) & & & \\
\frac{1}{2} & \frac{1}{2}\varphi_1\left(-\frac{hL}{2}\right) - a_{11} & a_{11} & & \\
\frac{1}{2} & \frac{1}{2}\varphi_1\left(-\frac{hL}{2}\right) - a_{21} - a_{22} & a_{21} & a_{22} & \\
\hline
1 & \varphi_1 - a_{31} - a_{32} - a_{33} & a_{31} & a_{32} & a_{33} \\
1 & \varphi_1 - \frac{67}{9}\varphi_2 + \frac{52}{3}\varphi_3 & 8\varphi_2 - 24\varphi_3 & \frac{26}{3}\varphi_3 - \frac{11}{9}\varphi_2 & a_{43} \ a_{44}
\end{array}$$

$$\begin{aligned}
\varphi_i &= \varphi_i(-hL) \\
a_{11} &= \frac{3}{2}\varphi_2\left(-\frac{hL}{2}\right) + \frac{1}{2}\varphi_2\left(-\frac{hL}{6}\right) \\
a_{21} &= \frac{19}{60}\varphi_1 + \frac{1}{2}\varphi_1\left(-\frac{hL}{2}\right) + \frac{1}{2}\varphi_1\left(-\frac{hL}{6}\right) \\
&\quad + 2\varphi_2\left(-\frac{hL}{2}\right) + \frac{13}{6}\varphi_2\left(-\frac{hL}{6}\right) + \frac{3}{5}\varphi_3\left(-\frac{hL}{2}\right) \\
a_{22} &= -\frac{19}{180}\varphi_1 - \frac{1}{6}\varphi_1\left(-\frac{hL}{2}\right) - \frac{1}{6}\varphi_1\left(-\frac{hL}{6}\right) \\
&\quad - \frac{1}{6}\varphi_2\left(-\frac{hL}{2}\right) + \frac{1}{9}\varphi_2\left(-\frac{hL}{6}\right) - \frac{1}{5}\varphi_3\left(-\frac{hL}{2}\right) \\
a_{33} &= \varphi_2 + \varphi_2\left(-\frac{hL}{2}\right) - 6\varphi_3 - 3\varphi_3\left(-\frac{hL}{2}\right) \\
a_{31} &= 3\varphi_2 - \frac{9}{2}\varphi_2\left(-\frac{hL}{2}\right) - \frac{5}{2}\varphi_2\left(-\frac{hL}{6}\right) + 6a_{33} + a_{21} \\
a_{32} &= 6\varphi_3 + 3\varphi_3\left(-\frac{hL}{2}\right) - 2a_{33} + a_{22} \\
a_{43} &= \frac{7}{9}\varphi_2 - \frac{10}{3}\varphi_3, \quad a_{44} = \frac{4}{3}\varphi_3 - \frac{1}{9}\varphi_2
\end{aligned}$$

Table 5: ERK43ZB tableau.

interpolation, and contour integrals) in relation to exponential RK methods is given in [8]. Instead of examining existing methods for computing matrix exponentials in greater detail, we propose a transformation to the equation such that the matrix in the term that is treated exactly by the ERK method is diagonal.

An important practical application of exponential integrators are PDEs containing a linear term Ly , where L is a Laplacian. If spectral transforms are used to convert spatial derivatives to algebraic expressions, the Laplacian becomes a diagonal matrix. Calculating the exponential of a diagonal matrix is straightforward to implement and computationally inexpensive. To avoid loss of accuracy due to finite numerical precision, truncations of Taylor series should be used when evaluating $\varphi_k(x)$ near 0 for $k > 0$ [1].

Other applications use finite differences to approximate the Laplacian as a nondiagonal discretized spatial operator. In these cases, the difficulty of accurately computing the various matrix φ_k functions has discouraged many

researchers from using adaptive exponential integrators. Recognizing the computational advantages of the diagonal case, it would seem reasonable when L is diagonalizable to compute a one-time change of basis that diagonalizes L ; that basis can then be reused for computing matrix functions of $c_j h L$ for arbitrary values of h . However, diagonalization is well known to become numerically unstable when eigenvalues coalesce. Moreover, not all matrices are diagonalizable. Instead of trying to diagonalize L , one can find its Schur decomposition

$$L = UTU^\dagger, \quad (22)$$

where U^\dagger denotes the conjugate transpose of the *unitary* matrix U (so that $U^\dagger = U^{-1}$) and T is an upper triangular matrix. Furthermore, we can write $T = D + S$, where D is a diagonal matrix and S is a strictly upper triangular matrix. Equation (21) becomes

$$\frac{dy}{dt} + U(D + S)U^\dagger y = F(t, y). \quad (23)$$

On multiplying by U^\dagger on the left we obtain

$$\frac{d(U^\dagger y)}{dt} + (D + S)U^\dagger y = U^\dagger F(t, y), \quad (24)$$

or, in terms of the transformed variable $Y = U^\dagger y$,

$$\frac{dY}{dt} + DY = U^\dagger F(t, UY) - SY, \quad (25)$$

By applying this transformation, we avoid working with exponentials of a full matrix in favour of exponentials of a diagonal matrix. The main trade-off is that we have to compute the Schur decomposition for the matrix L , but that is only done once and the longer the interval for the time integration, the more worthwhile this investment becomes. The second drawback is that some part that could have been treated exactly is now treated numerically and this could contribute to the overall error. In addition, we have to do two matrix multiplications at each step because the nonlinearity $F(t, y)$ is evaluated in the initial space. Although the efficiency gained in calculating the φ_k functions is more than enough to compensate for the drawback of two added multiplications per step and the potential of added numerical error, there is another advantage to implementing exponential RK methods in this way. The φ_k functions are now diagonal matrices and can thus be stored as vectors. This is a large improvement in memory usage as even for sparse matrices L , the matrix φ_k functions are general full matrices requiring extra storage. Furthermore, the ERK methods (and classical RK methods) work by multiplying the weights of the method by previously computed approximations of the vector y . In the case of ERK methods, the weights are linear combinations of matrix functions and hence matrices themselves. By implementing the Schur decomposition and being able to work with weights that are diagonal matrices, we have replaced all

the needed matrix-vector multiplications with computationally cheap vector dot products.

With the optimization afforded by Schur decomposition, the use of embedded ERK methods for step size adjustment becomes computationally viable, even when L is a nondiagonal matrix. An adaptive exponential method requires recalculating the weights (and corresponding φ_k functions) every time that the step size is adjusted. However, since these are now functions of diagonal matrices, there is no longer a huge computational cost to bear. As in the case of fixed step size, the Schur decomposition of L only needs to be performed once, so depending on the duration of the integration, the cost of the decomposition will typically be negligible.

Since many matrices encountered in practice are normal, the following result shows in these cases that the Schur decomposition technique not only removes linear stiffness from the problem, but will still handle the linear term exactly (since $S = 0$).

Theorem 1 *The triangle matrix in the Schur decomposition of a normal matrix is diagonal.*

Proof Assume L is a normal matrix:

$$LL^\dagger = L^\dagger L. \quad (26)$$

The Schur decomposition of L and L^\dagger are

$$L = U^\dagger T U \quad \text{and} \quad L^\dagger = U^\dagger T^\dagger U, \quad (27)$$

where T is a triangular matrix and U is a unitary matrix, so that $U^\dagger = U^{-1}$. Hence

$$U^\dagger T U U^\dagger T^\dagger U = U^\dagger T^\dagger U U^\dagger T U, \quad (28)$$

which reduces to

$$T T^\dagger = T^\dagger T. \quad (29)$$

This means that the triangular matrix T resulting from the Schur decomposition of L is normal. An inductive argument shows that it must then be diagonal [12].

In the general case, the strictly upper triangular matrix S resulting from the Schur decomposition will be non-zero. We now show that the term Sy does not incorporate any of the stiffness inherent in the linear term Ly . On defining the integrating factor $I(t) = e^{tD}$ and $\tilde{y}(t) = I(t)y(t)$, we can transform (25) in the autonomous case to

$$\frac{d\tilde{y}}{dt} = I(t)U^\dagger F(U I^{-1}(t)\tilde{y}) - \tilde{S}\tilde{y}, \quad (30)$$

where $\tilde{S} = I(t)S I^{-1}(t)$ is an $m \times m$ strictly upper triangular matrix. For systems of the form (21) where the stiffness only enters through the linear term Ly and not through $F(y)$, the first term on the right-hand side of (30) will

not contribute any additional stiffness. To analyze (30) we first consider the case $F = 0$, when it reduces to the triangular system of equations

$$\frac{d\tilde{y}_i}{dt} = \sum_{j=i+1}^m \tilde{S}_{ij}\tilde{y}_j \text{ for } i = 1, \dots, m-1 \quad \text{and} \quad \frac{d\tilde{y}_m}{dt} = 0, \quad (31)$$

which can be solved recursively to obtain the general solution as a polynomial in t . Recalling that stiffness arises only when nearby solution curves approach the solution curve of interest at exponentially fast rates, we deduce that since polynomials cannot approach each other exponentially fast, the system of equations is not stiff. Such ODE systems can even be solved exactly by a classical Runge–Kutta method whose degree is greater than or equal to the degree of each of the solution polynomials. By linear superposition, it follows that (30) is not stiff even when F is linear and, in particular, when F is constant. That is, all of the linear stiffness in (25) is contained within the diagonal term DY .

5 Examples and applications

Let us have a look at an example where the matrix L is upper triangular. First, we will solve the system by treating the full linear term by an exponential RK method. Then, we will split L into the sum of a diagonal matrix D and a strictly upper triangular matrix S , allowing us to treat the diagonal term exactly and the rest numerically. Consider the system

$$\frac{dy}{dt} = -Ly = -Dy - Sy, \quad (32)$$

where

$$D = - \begin{bmatrix} a & 0 & 0 \\ 0 & d & 0 \\ 0 & 0 & f \end{bmatrix}, S = - \begin{bmatrix} 0 & b & c \\ 0 & 0 & e \\ 0 & 0 & 0 \end{bmatrix} \quad (33)$$

and the eigenvalues a , d , and f of L are distinct. The general solution of this system of ODEs is

$$\begin{bmatrix} y_1 \\ y_2 \\ y_3 \end{bmatrix} = \begin{bmatrix} k_1 e^{-at} + \frac{bck_3 e^{-ft}}{(f-a)(f-d)} + \frac{bk_2 e^{-dt}}{d-a} + \frac{ck_3 e^{-ft}}{f-a} \\ k_2 e^{-dt} + \frac{ek_3 e^{-ft}}{f-d} \\ k_3 e^{-ft} \end{bmatrix}, \quad (34)$$

where the constants k_1 , k_2 , and k_3 are fixed by the chosen initial condition. This algebraic example allows us to run many tests with ease, say

$$L = - \begin{bmatrix} 1 & 2 & 7 \\ 0 & 75 & 8 \\ 0 & 0 & 15 \end{bmatrix}, \quad y(0) = \begin{bmatrix} 1 \\ 1 \\ 1 \end{bmatrix}. \quad (35)$$

For this problem, we compare in Figure 7 the error in **ERK4HO5M**, which is a matrix implementation of **ERK4HO5** [7] and **ERK4HO5V**, which is an implementation of the same method with only the diagonal part treated exactly. Here V stands for “vector” since the matrix in the linear term is taken to be the diagonal matrix D and M stands for “matrix” since the matrix in the linear term is the complete matrix L . The full matrix implementation **ERK4HO5M** is supposed to solve the problem exactly (since $F = 0$) but is still susceptible to floating point precision error. Both exponential methods behave as expected for large time steps. In comparison, we show how the classical RK4 method fails at large h . This small system of ODEs demonstrates the previous argument that stiffness is isolated to the diagonal term Dy .

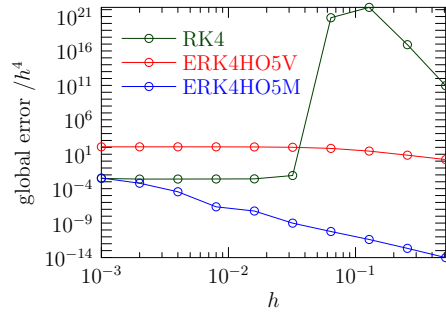


Fig. 7: Error at $t = 1$ when solving (35) with **ERK4HO5M**, **ERK4HO5V**, and RK4.

Consider Example 6.2 of [7]:

$$\frac{\partial y}{\partial t}(x, t) - \frac{\partial^2 y}{\partial x^2}(x, t) = \int_0^1 y(\bar{x}, t) d\bar{x} + \Phi(x, t), \quad (36)$$

for $x \in [0, 1]$ and $t \in [0, 1]$, subject to homogeneous Dirichlet boundary conditions, where the function Φ is chosen by substituting the specified exact solution

$$y(x, t) = x(1 - x)e^t \quad (37)$$

into (36). This problem can be transformed to a system of ODEs by performing a centered spatial discretization of the Laplacian and integral. We approximate the integral with the Simpson method, which in this case can be written as a matrix-vector multiplication. This means it is a linear term and hence could be fused with the linear term coming from the discretized Laplacian. Therefore, all exponential integrators could solve this problem exactly. Since treating numerically a part of the equation that can be treated exactly is not a fair comparison, we modify (36) to

$$\frac{\partial y}{\partial t}(x, t) - \frac{\partial^2 y}{\partial x^2}(x, t) = \int_0^1 y^4(\bar{x}, t) d\bar{x} + \Phi(x, t), \quad (38)$$

where again the function Φ is calculated by substituting (37) in (38). We discretized Problem (38) with 200 spatial grid points. As in [7], we calculate the matrix φ_k functions with the help of Padé approximants, along with scaling and squaring.

In Figure 8a, we plot the L^2 norm of the global error at $t = 1$ for the full discretized Laplacian matrix formulation of ERK4HO5 and the optimized implementation where the Laplacian is first reduced to a diagonal matrix via Schur decomposition. Figure 8b shows the same situation for the fourth-order estimate of ERK43ZB. Figure 9a and Figure 9b emphasize that even when the ERK4K and ERK4CM methods are applied to systems with a diagonal linear term, they can still suffer from order reduction.

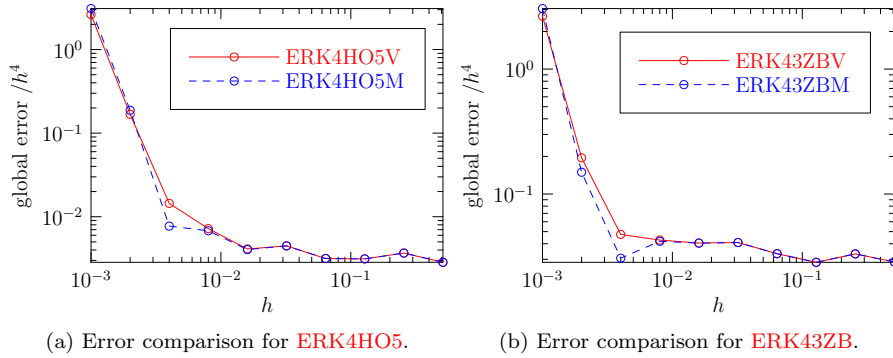


Fig. 8: Error comparison when solving (38) with and without the Schur decomposition.

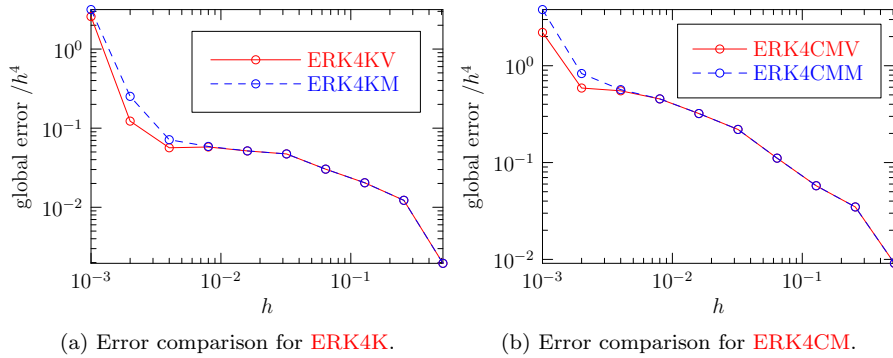


Fig. 9: Error comparison when solving (38) with and without the Schur decomposition.

To illustrate the impressive performance gain afforded by Schur decomposition, we considered the equation

$$\frac{\partial y}{\partial t}(x, t) - \frac{\partial^2 y}{\partial x^2}(x, t) = \frac{1}{1 + y(x, t)^2} + \Phi(x, t), \quad (39)$$

with Φ chosen so that the exact solution $y(x, t) = 10(1 - x)x(1 + \sin t) + 2$ is oscillatory rather than exponential. We integrated (39) from $t = 0$ to $t = 200$ using vector and matrix formulations of [ERK43ZB](#), with 3000 spatial points and a fixed time step of 0.3. The vector formulation [ERK43ZBV](#) was found to run about 117 times faster than the matrix formulation [ERK43ZBM](#), even after taking into account the cost of the Schur decomposition, which required about 50% of the total run time. Since [ERK43ZB](#) is a robust embedded method, it is even more meaningful to illustrate the practicality of Schur decomposition using adaptive time stepping on a large problem. For 10 000 spatial points, Schur decomposition took only about 7% of the total time required to integrate (39) from $t = 0$ to $t = 20\,000$.

6 Conclusion

Previous attempts at defining stiffness in the literature are inadequate. The quantitative definition of stiffness given in this work, which compares local Lyapunov exponents to curvature, provides a solid theoretical foundation for developing explicit numerical methods for stiff problems.

Explicit ERK methods are ideally suited to problems where the numerical stiffness comes from a linear term, as they allow for relatively large step sizes. Conventionally, ERK methods treat the linear term exactly. However, in this work we show that in the case where the linear term is a matrix, it is not necessary to treat the linear term exactly in order to remove linear stiffness.

ERK methods treat the linear term by calculating exponentials and related functions of the linear coefficient L . This is not a problem when L is just a number or if L is a diagonal matrix, but it is a computational burden when L is a general matrix (even if it is sparse). The Schur decomposition of the general matrix can be used to transform the linear coefficient to a triangular matrix. The diagonal part of the new linear term is treated exactly by the ERK method and the strictly triangular part is treated explicitly, together with the nonlinear term.

Schur decomposition is particularly useful for embedded ERK methods, because otherwise, every time that the step size is adjusted, matrix functions would have to be recalculated. With Schur decomposition, only functions of diagonal matrices need to be recalculated at each time step. Since the Schur decomposition algorithm only needs to be run once at the very beginning, this greatly optimizes embedded ERK methods and makes them a viable choice for high-performance computing.

Lastly, we would like to remark that while we have defined stiffness in general, exponential integrators can only circumvent linear stiffness. If there

is stiffness associated with the nonlinearity, one could (perhaps periodically) linearize the equation around a certain state [8]. However, the matrix L in the resulting linear part would not in general be diagonal and we would have to perform a Schur decomposition every time a linearization is performed. Another potential improvement is to account for the off-diagonal terms of the triangular matrix from the Schur decomposition by using optimized algorithms for calculating functions of triangular matrices.

Conflict of interest

The authors have no competing interests to declare that are relevant to the content of this article.

Data availability

All data generated or analyzed during this study is included in this published article.

References

1. Bowman, J.C.: Robust efficient routines to compute $\phi_n(x)$ for $n=1$ to 4. <https://github.com/dealias/triad/blob/master/phi.h> (2005)
2. Cartwright, J.H.: Nonlinear stiffness, lyapunov exponents, and attractor dimension. *Physics Letters A* **264**(4), 298–302 (1999)
3. Certaine, J.: The solution of ordinary differential equations with large time constants. *Mathematical methods for digital computers* **1**, 128–132 (1960)
4. Cox, S., Matthews, P.: Exponential time differencing for stiff systems. *J. Comp. Phys.* **176**, 430–455 (2002)
5. Curtiss, C.F., Hirschfelder, J.O.: Integration of stiff equations. *Proceedings of the National Academy of Sciences* **38**(3), 235–243 (1952)
6. Higham, N.J.: *Functions of matrices: theory and computation*. SIAM (2008)
7. Hochbruck, M., Ostermann, A.: Explicit exponential Runge–Kutta methods for semi-linear parabolic problems. *SIAM J. Numer. Anal.* **43**, 1069–1090 (2005)
8. Hochbruck, M., Ostermann, A.: Exponential integrators. *Acta Numerica* **19**, 209–286 (2010)
9. Krogstad, S.: Generalized integrating factor methods for stiff pdes. *Journal of Computational Physics* **203**(1), 72–88 (2005)
10. Lambert, J.D.: *Numerical methods for ordinary differential systems: the initial value problem*. John Wiley & Sons, Inc. (1991)
11. Moler, C., Van Loan, C.: Nineteen dubious ways to compute the exponential of a matrix, twenty-five years later. *SIAM review* **45**(1), 3–49 (2003)
12. Prasolov, V.V.: *Problems and theorems in linear algebra*, vol. 134. American Mathematical Soc. (1994)
13. Zoto, T., Bowman, J.C.: Robust exponential Runge–Kutta embedded pairs. *SIAM J. Sci. Comput.* (2023). Submitted